

Supporting Information

Modulation of iron spin states in highly distorted iron(III)porphyrin: H-bonding interactions and implications for the hemoproteins

Dipankar Sahoo, Rakesh Mazumdar, Subhadip Pramanik, Sayantani Banerjee, Ranjan Patra,
and Sankar Prasad Rath*

X-ray Structure Solution and Refinement. Single-crystal X-ray data were collected at 100 K on a Bruker SMART APEX CCD diffractometer equipped with CRYO Industries low-temperature apparatus, and intensity data were collected using graphite monochromated MoK α radiation ($\lambda = 0.71073 \text{ \AA}$). The data integration and reduction were processed with SAINT software.¹ An absorption correction was applied.² The structure was solved by the direct method using SHELXS-97 and was refined on F2 by the full-matrix least-squares technique using the SHELXL-2018 program package.³ Non-hydrogen atoms were refined anisotropically. In the refinement, hydrogens were treated as riding atoms using SHELXL default parameters.

$[\text{Fe}^{\text{III}}(\text{TPPBr}_8)(\text{H}_2\text{O})_2]\text{ClO}_4$ and $\text{Fe}^{\text{II}}(\text{TPPBr}_8)(1\text{-MeIm})_2$ contain several severely disordered solvent molecules which could not be modelled properly due to weakly diffracting nature of the crystals and thus, the SQUEEZE routine of PLATON⁴ were used to remove such unbound and highly disordered solvent molecules (four THF and eight C₆H₆ molecules per unit cell for $[\text{Fe}^{\text{III}}(\text{TPPBr}_8)(\text{H}_2\text{O})_2]\text{ClO}_4$ and $\text{Fe}^{\text{II}}(\text{TPPBr}_8)(1\text{-MeIm})_2$, respectively) but the reported formula includes the solvent molecules.

$\text{Fe}^{\text{III}}(\text{TPPBr}_8)(\text{OCHMe}_2)$ [CCDC Number: 2247017]

SADABS (Bruker) was used for absorption correction. R(int) was 0.1191 before and 0.0361 after correction. Ratio of minimum to maximum apparent transmission: 0.247600. Lambda/2 correction factor = 0.0015.

Exposure time, 18 sec

$\text{Fe}^{\text{II}}(\text{TPPBr}_8)(1\text{-MeIm})_2$ [CCDC Number: 2247018]

SADABS(Bruker) was used for absorption correction. R(int) was 0.1440 before and 0.0485 after correction. Ratio of minimum to maximum apparent transmission: 0.328215. Lambda/2 correction factor = 0.0015.

Exposure time, 18sec

[Fe^{III}(TPPBr₈)(H₂O)₂]ClO₄ [CCDC Number: 2247019]

SADABS (Bruker) was used for absorption correction. R(int) was 0.0869 before and 0.0321 after correction. Ratio of minimum to maximum apparent transmission: 0.097427. Lambda/2 correction factor = 0.0015

Exposure time, 28 sec

[Fe^{III}(TPPBr₈)(MeOH)₂]ClO₄ [CCDC Number: 2247020]

SADABS (Bruker) was used for absorption correction. R(int) was 0.1071 before and 0.0667 after correction. Ratio of minimum to maximum apparent transmission: 0.735336. Lambda/2 correction factor = 0.0015.

Exposure time, 15sec

- 1 SAINT+, 6.02 ed., Bruker AXS, Madison, WI, 1999.
- 2 G. M. Sheldrick, SADABS, Bruker AXS Inc., Madison, WI, 2000.
- 3 G. M. Sheldrick, SHELXL: Program for Crystal Structure Refinement, University of Göttingen, Göttingen, Germany, 2018.
- 4 A. L. J. Spek, *Appl. Crystallogr.*, 2003, **36**, 7.

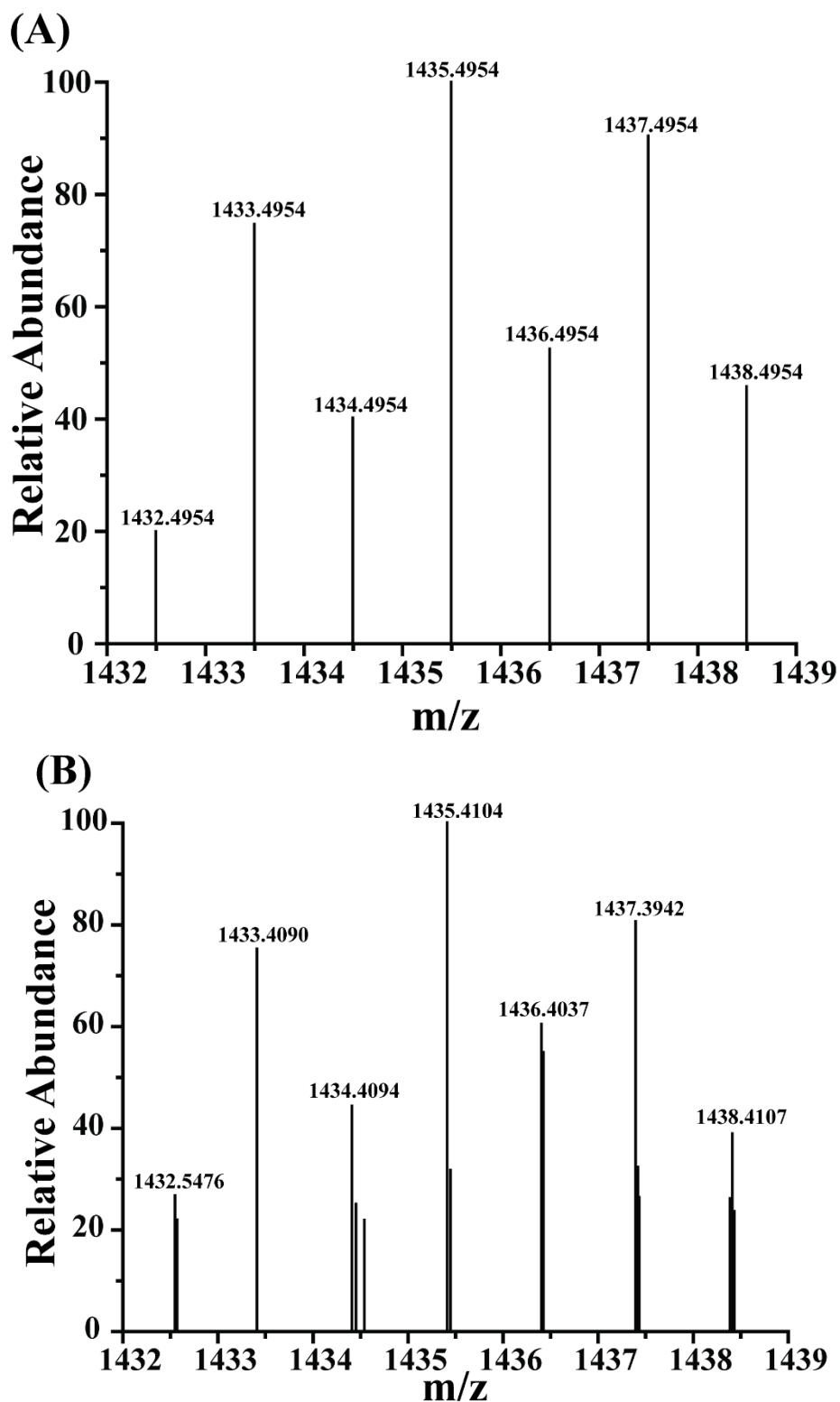


Figure S1. Isotopic distribution pattern of $[\text{Fe}^{\text{III}}(\text{TPPBr}_8)\text{Cl} + (\text{CH}_3\text{CN})_2 + \text{H}_2\text{O} + \text{H}]^+$, (A) simulated, and (B) experimental ESI mass spectrum displaying m/z peak at 1435.4104 (positive-ion mode).

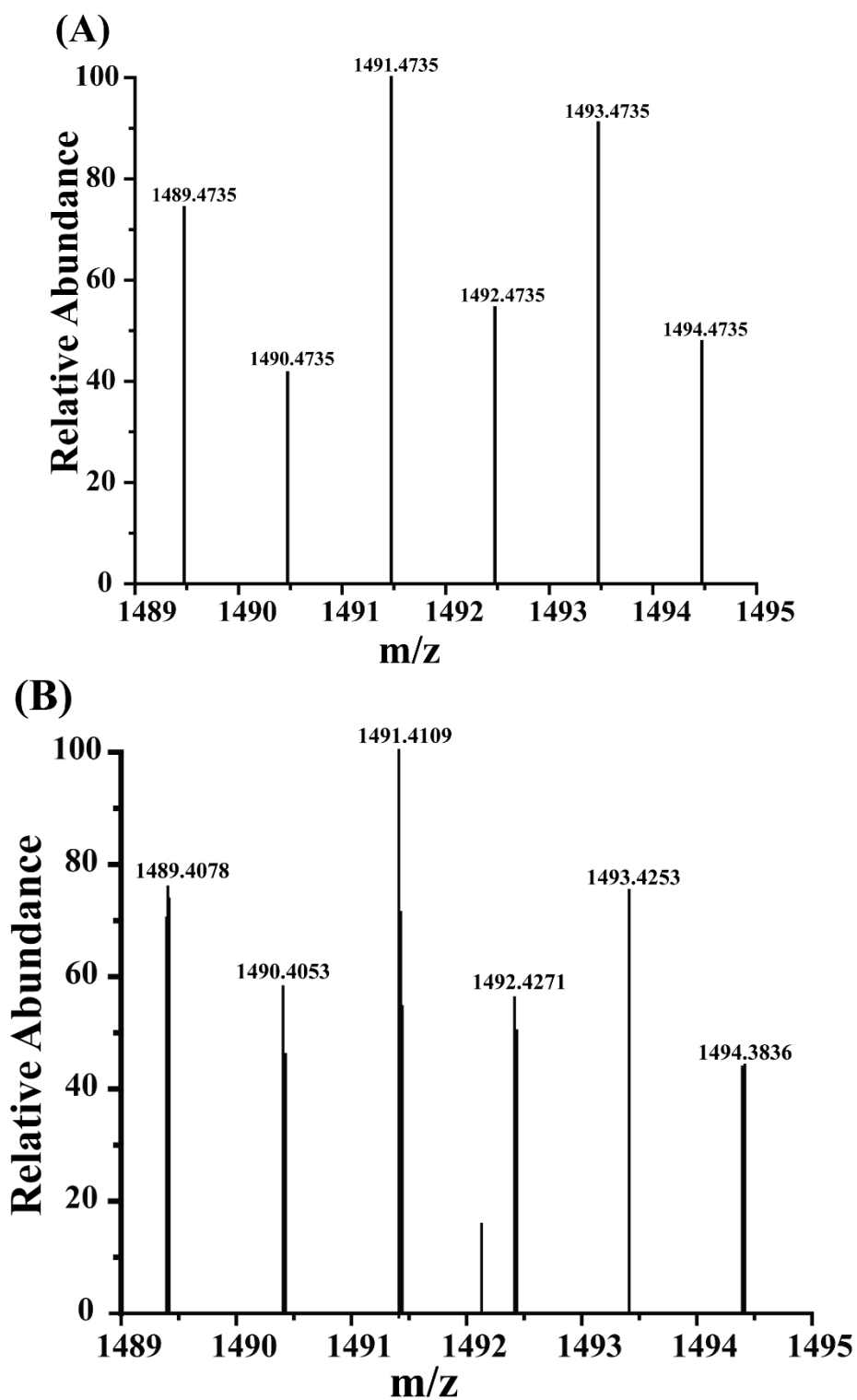


Figure S2. Isotopic distribution pattern of $[\text{Fe}^{\text{III}}(\text{TPPBr}_8)\text{ClO}_4 + \text{PhCH}_3 + \text{H}]^+$, (A) simulated, and (B) experimental ESI mass spectrum displaying m/z peak at 1491.4109 (positive-ion mode).

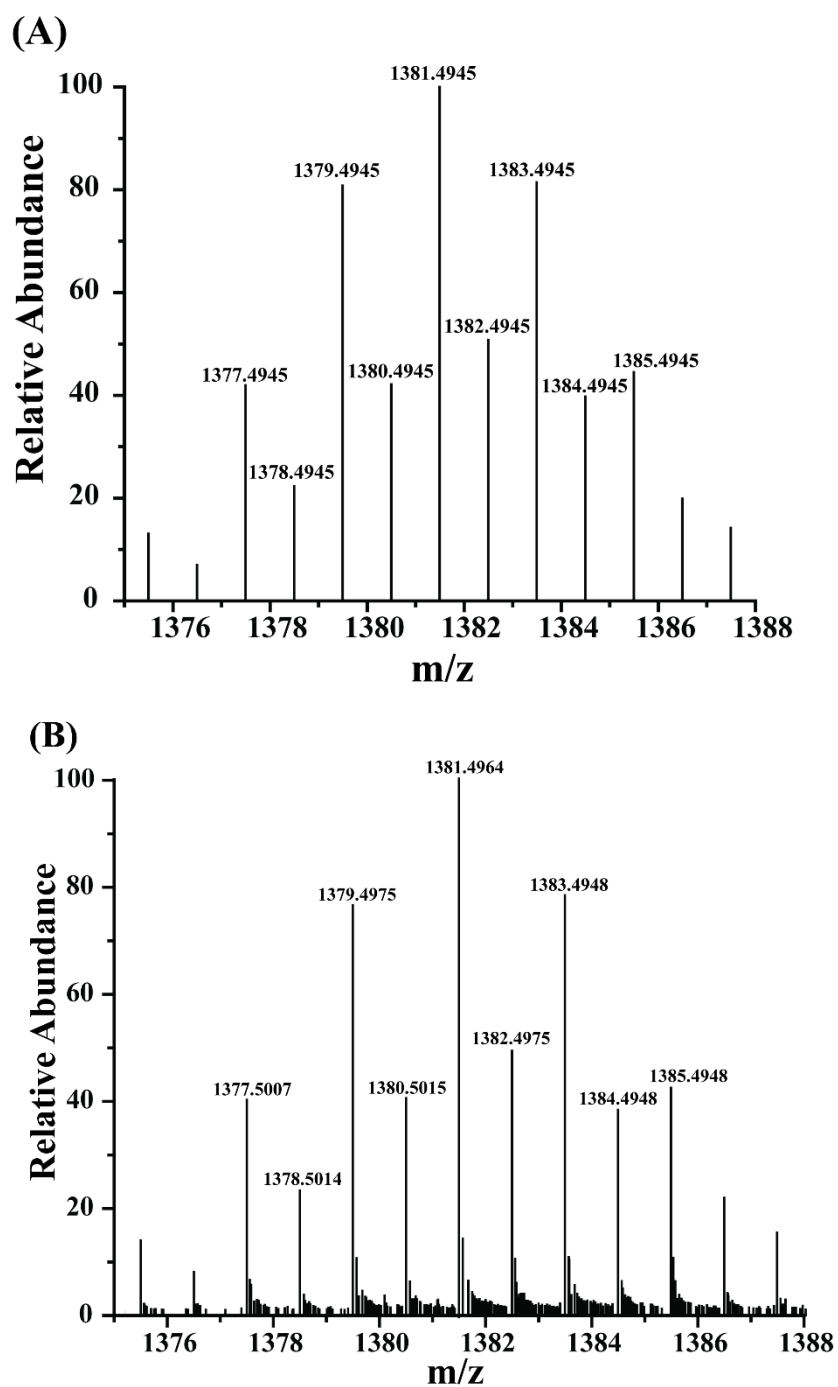


Figure S3. Isotopic distribution pattern of $[\text{Fe}^{\text{III}}(\text{TPPBr}_3)(\text{OCHMe}_2) + \text{Na}]^+$, (A) simulated, and (B) experimental ESI mass spectrum displaying m/z peak at 1381.4964 (positive-ion mode).

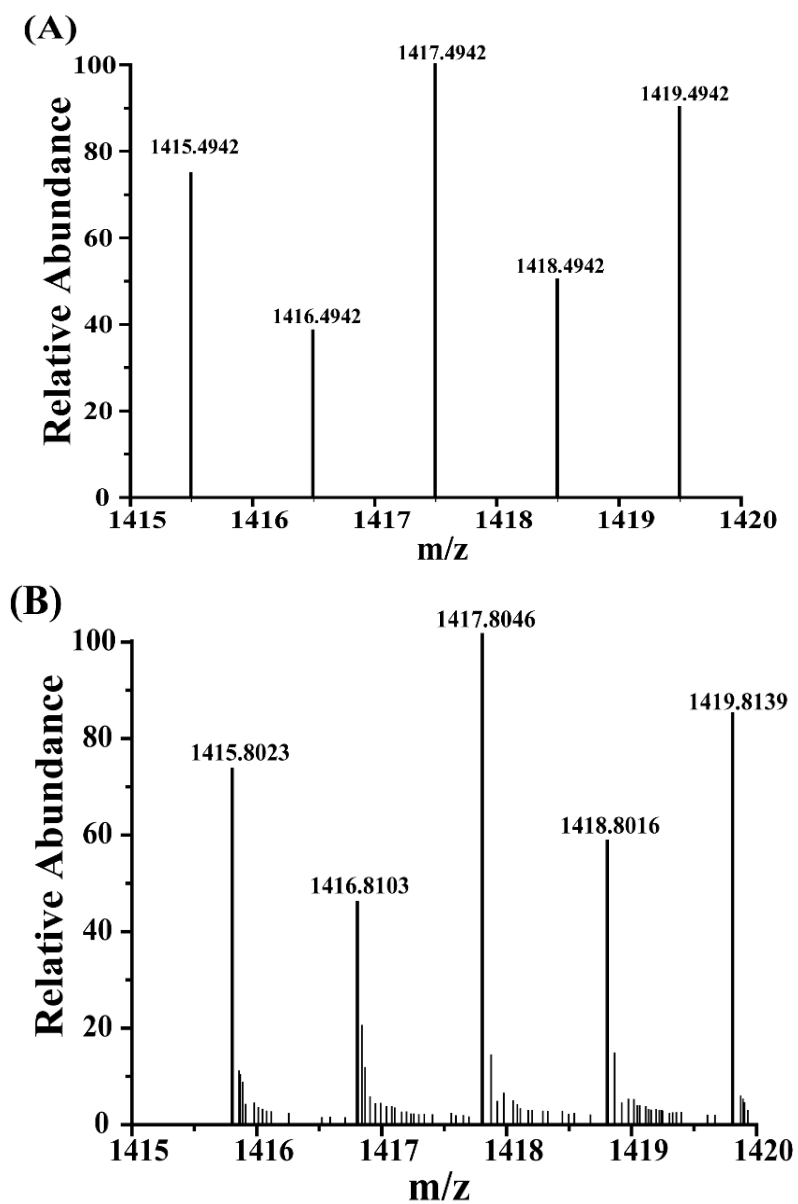


Figure S4. Isotopic distribution pattern of $[\text{Fe}^{\text{III}}(\text{TPPBr}_8)(\text{MeOH})_2 + (\text{H}_2\text{O})_3]^+$, (A) simulated, and (B) experimental ESI mass spectrum displaying m/z peak at 1417.8046 (positive-ion mode).

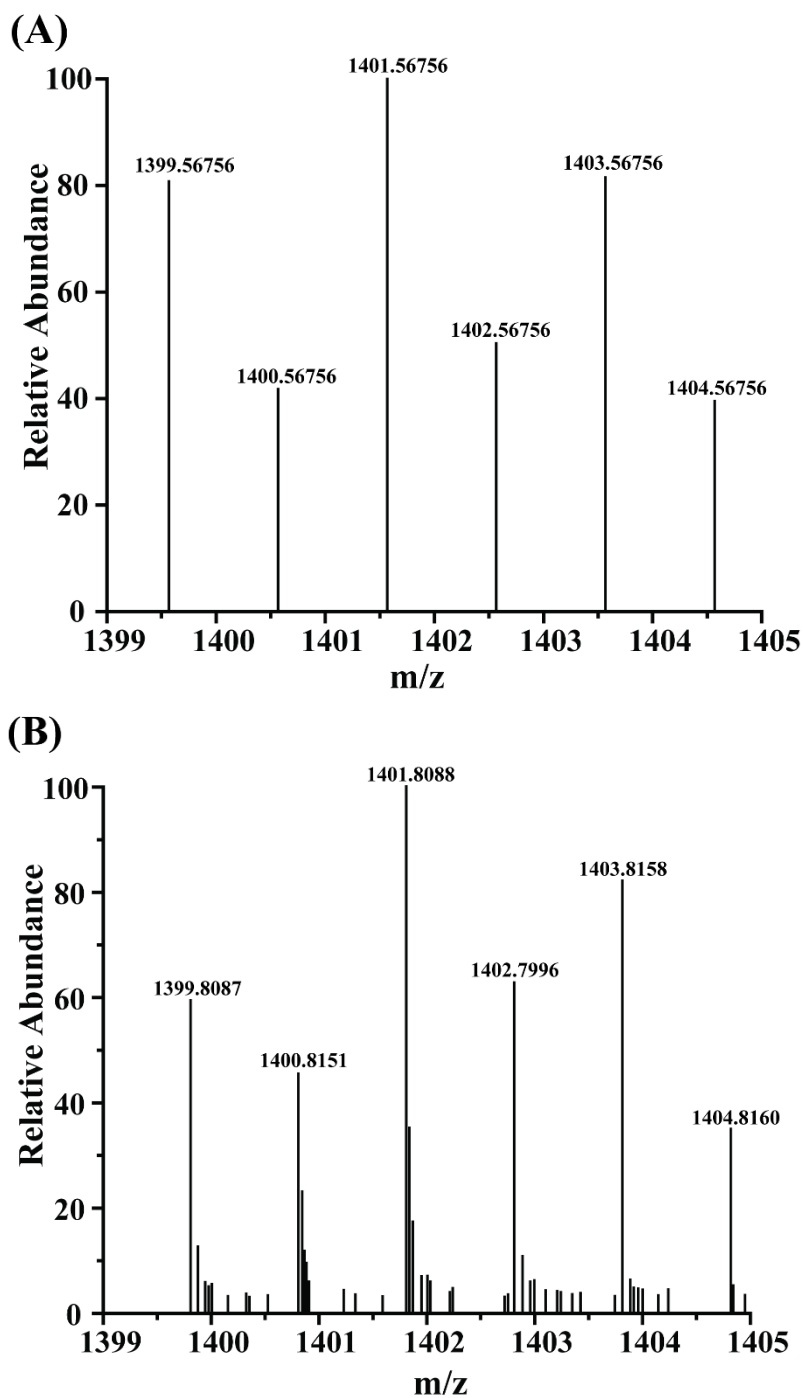


Figure S5. Isotopic distribution pattern of $[\text{Fe}^{\text{III}}(\text{TPPBr}_8)(\text{OH}_2)_2 + (\text{MeOH})_2 + \text{H}]^+$, (A) simulated, and (B) experimental ESI mass spectrum displaying m/z peak at 1401.8088 (positive-ion mode).

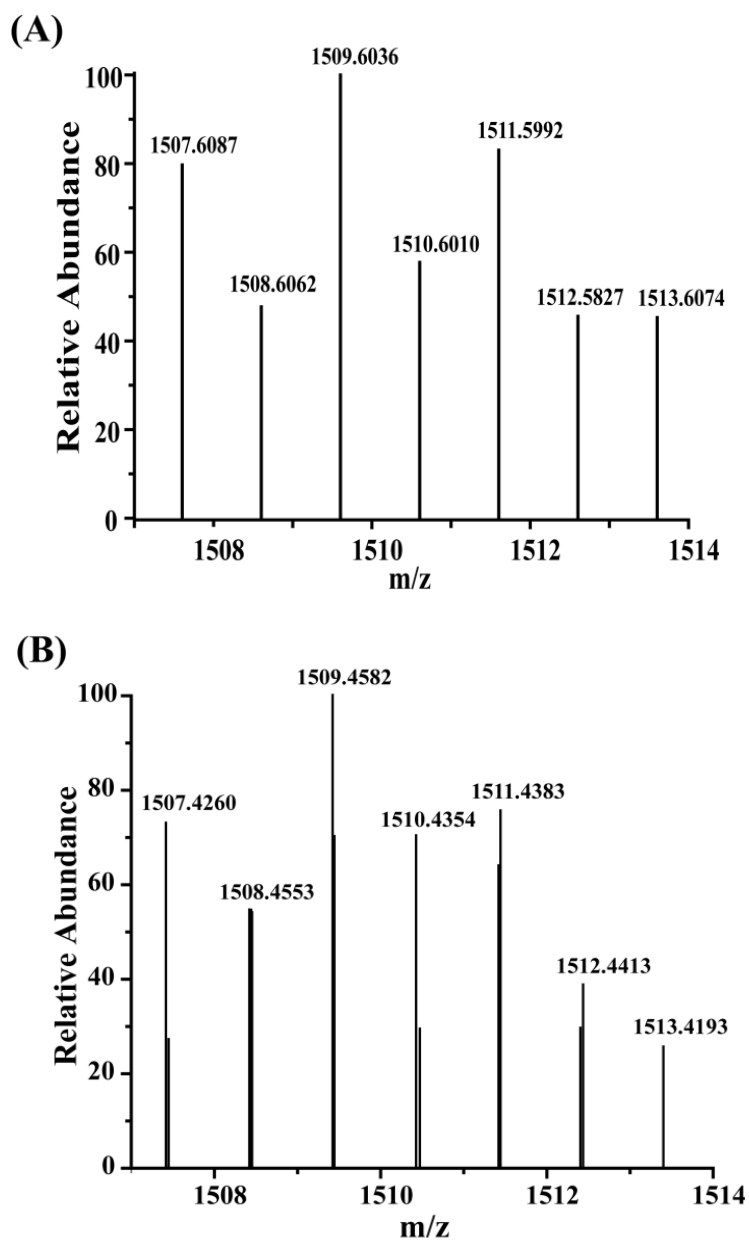


Figure S6. Isotopic distribution pattern of $[\text{Fe}^{\text{II}}(\text{TPPBr}_8)(1\text{-MeIm})_2 + \text{C}_2\text{H}_5\text{OH}]^+$, (A) simulated, and (B) experimental ESI mass spectrum displaying m/z peak at 1509.4582 (positive-ion mode).

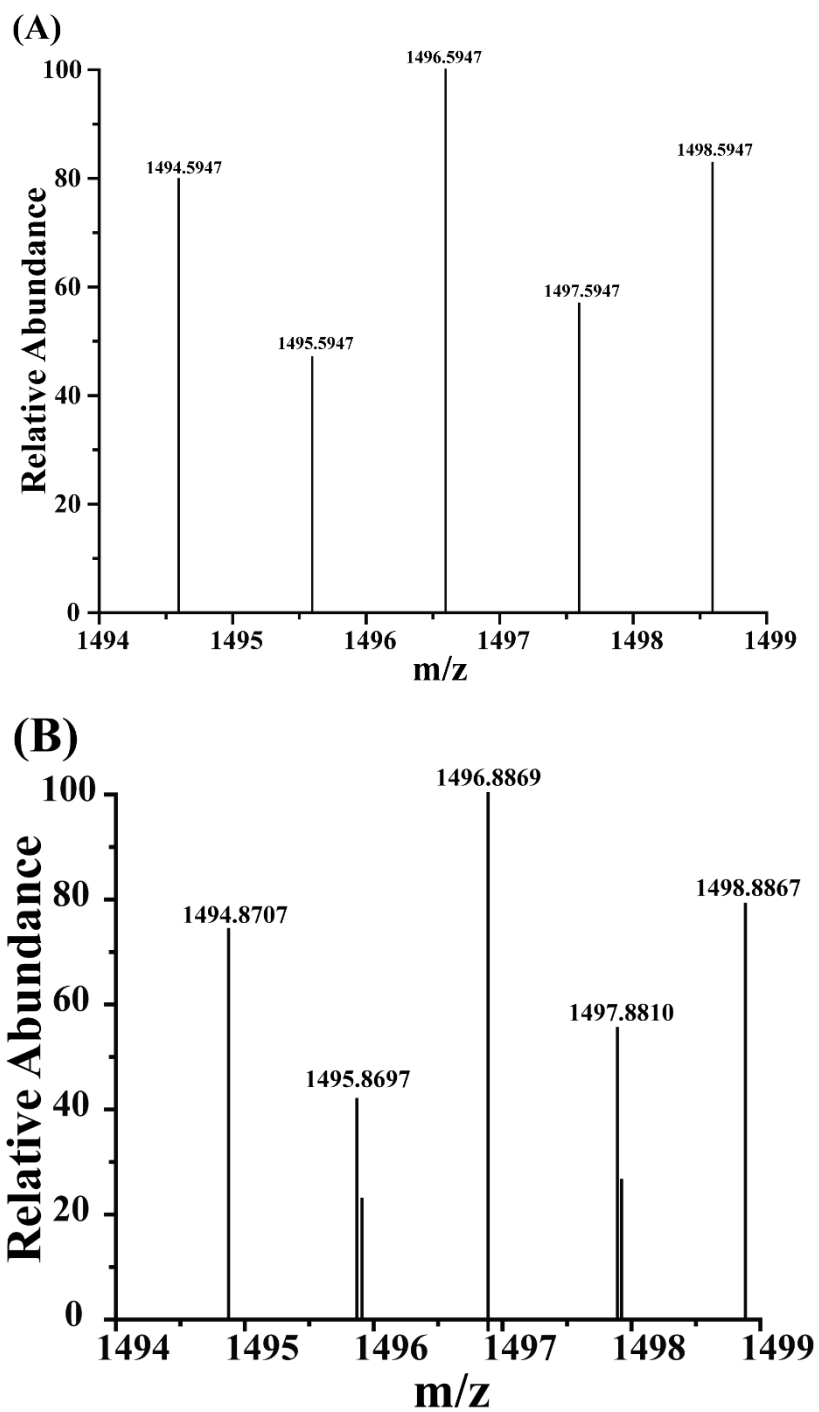


Figure S7. Isotopic distribution pattern of $[\text{Fe}^{\text{II}}(\text{TPPBr}_8)(4\text{-MeIm})_2 + \text{MeOH} + \text{H}]^+$, (A) simulated and (B) experimental ESI mass spectrum displaying m/z peak at 1496.8869 (positive-ion mode).